

Casimir Forces via Worldline Numerics: Method Improvements and Potential Engineering Applications

Klaus Aehlig¹, Helge Dietert², Thomas Fischbacher¹, and Jochen Gerhard³

¹ University of Southampton, Faculty of Engineering and the Environment,
Southampton, UK

² University of Cambridge, UK

³ Frankfurt Institute for Advanced Studies,
Institut für Informatik,
Goethe Universität Frankfurt, DE

November 10, 2018

Abstract

The string theory inspired Worldline Numerics approach to Casimir force calculations has some favourable characteristics that might make it well suited for geometric optimization problems as they arise e.g. in NEMS device engineering. We explain this aspect in detail, developing some refinements of the method along the way. Also, we comment on the problem of generalizing Worldline Numerics from scalars to photons in the presence of conductors.

1 Introduction

Casimir forces, i.e., electromagnetic forces arising due to quantum effects between uncharged conductors at distances much larger than characteristic atomic radii, have first been predicted via theoretical considerations in 1948 [1], and have since been verified experimentally to 1% accuracy [2]. While initially a fringe subject – albeit unfortunately one that drew considerable attention from pseudo-scientific authors – research interest in Casimir forces strongly increased in particular in the last decade, and a number of novel theoretical tools were developed [3, 4, 5, 6] that allow the study of the Casimir effect in considerably more involved situations (geometries, material properties, temperature) than earlier investigations. At present, one major obstacle to research is that Casimir force calculations often still are computationally very demanding. Nevertheless, the development of theoretical tools and methods must go hand in hand with progress in nanoscale manufacturing, for it is clear that a sound understanding of the role of Casimir forces in nano machines will become increasingly important as we learn to manufacture on shorter length scales.

One approach to the calculation of Casimir forces is based on the “Worldline approach” developed by Gies, Klingmüller, Langfeld and Moyaerts [7, 4, 8]. While this mostly has been used to study a simplified field theoretic model with massless scalars instead of vector gauge bosons (photons), and nowadays alternative methods are available to directly calculate electrodynamic effects even with frequency-dependent optical properties of materials [9, 10], the worldline approach is interesting for a number of reasons:

- Due to the probabilistic nature of the method, it is sometimes computationally comparatively cheap (depending on the geometry) to obtain a rough estimate of Casimir forces.
- With very little effort, the calculation can be modified in such a way that it simultaneously gives all the forces on a number of bodies, making it potentially attractive for problems requiring a geometric shape optimization approach.
- Finally, it is formulated in a way that is suggestive of a remarkably intuitive interpretation. This may manage to make this conceptually subtle quantum effect somewhat accessible to wider audiences not necessarily deeply familiar with quantum field theory. (One should compare this with the didactic problems related to the “mesomeric effect” in chemistry.)

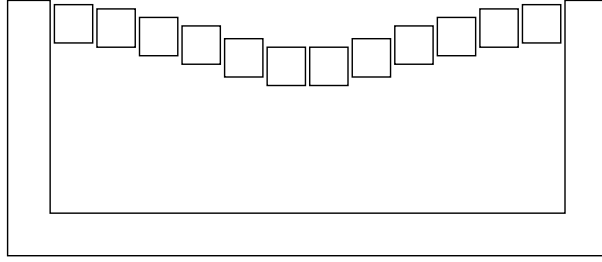


Figure 1: Beam bending under the influence of external forces and moments, a standard problem in Engineering, may be regarded as an energy minimization problem. Geometries such as the one shown above that involve bending beams at tens-of-nanometers length scales are presently being discussed as nanoelectromechanical memory devices [11]. Here, the beam also serves as a floating gate that allows electronic read-out of its mechanical state (upward bent or downward bent). Discretizing the beam into elements with one translational degree of motion, the nature of the Worldline numerics algorithm makes it easy to *simultaneously* calculate the Casimir forces on all elements with a computational effort less than one order of magnitude above the effort required to get a reliable estimate for the Casimir energy of the given configuration – *independent of the number of elements*. This is not easily achieved with a number of alternative methods to calculate Casimir forces.

In this article, we will focus mostly on the second item in the list above, which is elucidated in detail in Section 2.5. The key insight is that a deformable object, such as a beam bending under the influence of Casimir forces as shown in figure 1, when discretized into N elements (blocks) that are partially restricted in their relative motion, may require a certain computational effort, T processor-seconds, for a reasonable estimate of the Casimir energy of a given configuration, but will then always allow the simultaneous computation of Casimir forces (and moments) on *all* N elements in a way that requires at most $5T$ processor-seconds, *irrespective of the number of bodies* N .

2 Computational Methods

In contradistinction to other approaches, Worldline Numerics is remarkably simple to implement in a computer program, requiring almost no advanced software library infrastructure to deal with issues such as parallel sparse matrix linear algebra, multipole moments, or large matrix eigenvalues. Still, there are a number of useful improvements of the basic method that help to ensure making effective use of computational resources. As these are often linked to one another, it makes sense to address them in a coherent fashion.

2.1 Monte Carlo integration over Loops

The Casimir energy for a static geometry that can be modeled by a position-dependent potential $V(x)$ is given as the quantum effective action per unit time:

$$E_{\text{Casimir}} = \frac{\Gamma[V]}{\int_{\tau=\tau_-}^{\tau=\tau_+} d\tau} \quad (1)$$

The “Worldline Numerics” approach by Gies, Langfeld, and Moyaerts [12] is based on re-writing the logarithm in the effective action as an integral $\ln(p/q) \rightarrow \int_0^\infty \frac{dT}{T} (\exp(-px) - \exp(-qx))$ and re-expressing the operator trace as a Feynman path integral. This leads, for a real scalar field of mass m interacting only with the external potential V , to an expression for the effective action that is numerically tractable via Monte Carlo methods. The key expression from [12], which we repeat here for the convenience of the readers, is:

$$\Gamma_\Lambda[V] = -\frac{1}{2} \frac{1}{(4\pi)^2} \int_{1/\Lambda^2}^\infty \frac{dT}{T^3} e^{-m^2 T} \int d^4x \left[\langle W_V[y; x, T] \rangle_y - 1 \right] \quad (2)$$

where an UV cut-off regulator Λ has been introduced. Here, the expectation value $\langle \cdot \rangle_y$ is the ensemble average over all closed loop (c.l.) gaussian random walks $y : [0; 1] \mapsto \mathbb{R}, y(0) = y(1)$ of “Wilson loops” re-scaled to proper time T . Let the statistical weight of the loop y be

$$p[y] = \exp \left(- \int_{t=0}^{t=1} dt \dot{y}(t)^2 / 4 \right) \quad (3)$$

then:

$$\langle W_V[y; x, T] \rangle_y = \frac{\int_{y \text{ c.l.}} \mathcal{D}y W_V[y; x, T] p[y]}{\int_{y \text{ c.l.}} \mathcal{D}y p[y]} \quad (4)$$

where W_V depends on the *path* y and on position shift x and proptime T :

$$W_V[y; x, T] = \exp\left(-T \int_{t=0}^{t=1} dt V(x + \sqrt{T}y(t))\right). \quad (5)$$

From this expression for the effective action of a free scalar interacting with a potential, Casimir forces can be obtained by using the position dependency of the potential $V(x)$ to model the geometry, and calculating energy changes associated with changes to the geometry.

While the applicability of this model for the calculation of real Casimir forces is questionable (even for perfect conductors) as the physics of photons is quite different from that of a scalar field, the remarkable conceptual simplicity of the above expressions certainly warrants a deeper investigation of its properties and potential utility, for it might actually allow a (yet undiscovered) generalization to the photon case. For the electromagnetic case, one would naturally want to start with investigations of perfect conductor surfaces, and the (obvious) scalar pendant of this is a potential $V(x)$ that suppresses all quantum fluctuations *inside* the given bodies. It is not difficult to see that one may alternatively restrict the potential to have non-zero values only close to the surfaces of bodies, taking

$$V(x) = \lambda \int_{\Sigma} d^2\sigma \delta^3(x - x_{\sigma}) \quad (6)$$

and considering the limit $\lambda \rightarrow \infty$. Then, $W_V[y; x, T]$ reduces to:

$$\exp\left[-T \int_0^1 dt V(x + \sqrt{T}y(t))\right] = \begin{cases} 1 & \text{Loop pierces a surface} \\ 0 & \text{Loop does not pierce a surface.} \end{cases} \quad (7)$$

Substituting $s = \sqrt{T}$ to eliminate the square root, and using translation invariance of the integral to ensure all loops have center of gravity at the origin, the expression for the geometry-dependent regularized Casimir energy then is:

$$\Gamma_{\Lambda} = -\frac{1}{(4\pi)^2} \int_{1/\Lambda}^{\infty} \frac{ds}{s^5} \langle \Theta_V(sy, x) \rangle_y \quad (8)$$

where the mean value is over all unit loops, sy is the loop $y(t)$ scaled pointwise around its center of gravity \bar{y} by the factor s , and

$$\Theta_V(sy, x) = \begin{cases} 0 & \text{Loop does not pierce a surface} \\ 1 & \text{Loop pierces a surface.} \end{cases} \quad (9)$$

The problem with this approach is that the Casimir energy attributed to the surface of any single body goes to infinity as we send the energy regulator Λ to infinity, due to the contribution from very short loops close to the surface. (This is, of course, a non-physical artefact related to the “geometry much larger than atomic scales” approximation.) In order to predict Casimir forces between different objects we are only interested in the dependency of the energy on the relative position of these objects. Therefore, it makes sense to modify this scheme in a way that (i) the contribution of each loop is taken into account relative to a configuration in which all objects are at infinite separation from one another, and (ii) the Casimir energy contribution attributed to loops piercing only one object surface (hence, “belonging” to that object) is taken as zero.

Consider n objects with potentials V_1, \dots, V_n . Then the total potential is $V = V_1 + V_2 + \dots + V_n$ and we use the freedom to shift the absolute energy level to define the “interaction Casimir energy” E as in [12] as the energy difference relative to a configuration in which every body is at an effectively infinite distance from every other body:

$$E = (\Gamma[V] - \Gamma[V_1] - \Gamma[V_2] - \dots - \Gamma[V_n]) / \Delta\tau \quad (10)$$

Using this, we get

$$E = -\frac{1}{(4\pi)^2} \int_{1/\Lambda}^{\infty} \frac{ds}{s^5} \langle \Theta(sy, x) \rangle_y \quad (11)$$

with Θ given by

$$\Theta(sy, x) = \begin{cases} 0 & \text{Re-scaled loop does not pierce any surface} \\ 1 - n & \text{Re-scaled loop pierces the surfaces of } n \geq 1 \text{ objects} \end{cases} \quad (12)$$

If n objects come close to one another, every loop that pierces all of them can be regarded as the image of n loops, each to be considered as being attached to (and moving with) that body.

Hence, when objects are in proximity, we count a loop *once* that would have been counted n times instead for separated objects. (Note that the counting weight of both a loop that pierces no surface, and a loop that pierces only one surface, is zero.) If the objects are now spatially separated the integral $\int_{1/\Lambda}^{\infty} \frac{ds}{s^5} \langle \Theta(sy, x) \rangle_y$ is finite and well behaved for $\Lambda \rightarrow 0$, so we can safely set $\Lambda = 0$. One is easily convinced that this is indeed the correct expression by considering a simple geometry (such as two parallel flat slabs) and requesting that the Casimir force does not change if one object is instead thought of as being made of two adjacent bodies. The counting weights are dictated by the convention for the “zero energy” configuration.

For each loop y , the weight Θ , as a function of the re-scaling factor s , is piece-wise constant. The s -integral hence can easily be performed analytically. Rather than being only a convenient simplification that saves computing time, this property plays a crucial role for the efficient simultaneous computation of multibody forces, cf. Section 2.5.

2.2 Loop Generation

When trying to evaluate Equation 11, one naturally would try to discretize the loop as consisting of a finite number of straight sections. Taking the procedure literally, the presence of complicated curved geometries would mandate computationally fairly expensive ray-surface intersection checks. In many cases, a better investment of the computational effort may be to instead make the number of discretization points on the loop sufficiently large to ensure that simple inside/outside checks applied to each point give a reasonably close approximation. Still, generic ray/surface intersection checks can become useful, especially if the complicated multiple integral in Equation 11 (over loop shapes, loop sizes, and loop centers of gravity) can partially be evaluated by analytic, or rather semi-analytic means that involve numerical approximation of integral boundaries. This is relevant for the discussion in Section 2.4, and may make major computational improvements of the method possible. In this context, we want to point out the existence of advanced algorithms useful for ray/surface intersection problems, such as Comba and Stolfi’s Affine Arithmetic [13, 14].

In order to generate a properly distributed random sample of loops, we first generalize the problem to finding a process that produces piecewise straight paths with gaussian length distribution (of given standard deviation) for a given starting and end point (not necessarily coincident). This problem can be re-phrased as finding pairs of such paths, each with its own starting point but at first without any constraint on their endpoints, and imposing the condition that they meet at their endpoints. Concatenating the first path to the reverse of the second solves the problem of finding a path with the correct distribution between two given points. One easily sees that the distribution of the midpoint is still gaussian (being the product of two gaussian distributions). Hence, we can sample a loop by recursively sampling an intermediate point in the interval between a given start and end point.

This method, known as the “d (‘doubling’) loop algorithm” [15], manages to generate closed loops with the desired distribution with very little effort. A slight problem of this approach is that it only generates loops for which the number of vertices is a power of two, but as one usually is only interested in getting below a given resolution, and this method will at worst require an effort too large by a factor 2, this is practically irrelevant. Nevertheless, the reasoning presented above is readily generalized to non-equal subdivisions (e.g. 1/3 plus 2/3), and from there to also allow recursive subdivision into other numbers of parts, but this is typically not needed. In order to generate a loop containing 10 points using the extended d-loop method, one would first determine the opposite point (point #6) of the starting point (point #1), then for both arcs use a 2 : 3 split of the associated variance budget and work out the gaussian distribution of the corresponding intermediate point’s position. Sub-division of the arc of length 2 is straightforward, while the length 3 arc would first be split 1 : 2 using the same approach.

Rather than choosing starting points randomly in space and then determining the location of the halfway-round-the-loop point, it makes sense to perform stratified spatial sampling on a lattice. To do so, we choose the first point to be the lattice point and take the halfway point to be gaussian distributed with mean the first point and standard deviation a characteristic length. We then continue sampling a loop of that length and later scale it around the midpoint between the first point and the halfway point appropriately to obtain a unit loop. In that way, the midpoint is gaussian distributed around the lattice point with a given length scale.

If we want unbiased integration by taking loops for each lattice point, the lattice points have to be representative for loops sampled in their vicinity, with a characteristic length being that of the grid. This is certainly true if the grid is fine compared to any characteristic length of the geometry. However, the same can be achieved for arbitrary grids, if we take the characteristic length in the just described stratified sampling to be that of the grid.

A different kind of lattice effects has to be taken into account for methods computing a force as a difference in energy for two given geometries. Such methods would typically put a fixed set of loops on each lattice point and add up their energy contributions. Then they would do the same for the same geometry with one object moved in a particular direction. The difference in energy is then proportional to the force component on the moved object in the given direction.

To focus on the net effect, as we do with symmetries (see 2.7), one typically would use the same set of loops for both geometries. Also, to have for each loop a corresponding shifted loop, the amount the object is moved has to be a multiple of the grid length (in this direction). While doing otherwise would not necessarily yield a bias, doing so significantly improves the convergence speed of this method.

For our purposes, we typically only ask simple questions about each loop, such as “which objects does it hit?”, or (at most) “For what scaling intervals does this loop, centered at x_{cm} but re-scaled in size, hit object O_n ?”. In order to answer these, only very little information needs to be stored when visiting the loop point by point. So it is possible to implement the relevant algorithms in such a way that the loop is generated on the fly, and we never have to store the entire loop in memory – the number of points we have to remember is about the binary logarithm on the loop length. This yields an algorithm with a very small memory footprint and attractive characteristics for computing architectures that emphasize a high degree of parallelism between very simple cores.

2.3 Numerical Integration over the Scaling Factor

One approach to obtain energies—and so ultimately, by comparing energies for different geometric configurations, forces—is to directly evaluate the integral in Equation 11 numerically. Naively, one would have to, for various values of s , estimate $\langle \Theta(sy, x) \rangle_y$ and summing up. Since the order of summing up does not matter, we can as well compute the expectation value of the following process.

Choose s uniformly at random from the interval $[a, b]$. Randomly generate a loop sy of size s and count $(1 - n)/s^5$ if the loop hits $n \geq 2$ objects, and 0 otherwise.

Here $[a, b]$ is an interval big enough so that integrating over that interval does not differ noticeably from integrating over all positive reals.

Looking at that random process more closely, one notes that the information about the random loop we use is the number of objects it hits. We have to pay particular attention to short loops that are just long enough to barely touch multiple objects, for they give the largest contribution to the sum. One should note that it is not possible to attribute a useful physical meaning to absolute differences in loop scaling factors s : for a loop that hits (at least) two objects, the effect of changing s to $s + 0.1$ very much depends on what the magnitude of s is. As relative changes of the scaling factor hence are more important than absolute changes, we much prefer a distribution, when sampling loops, that handles all orders of magnitude equally. In other words, we prefer a distribution where the logarithm of s is uniformly distributed on $[\ln(a), \ln(b)]$.

When changing the distribution of s , we also have to transform the weight attributed to each sample accordingly. Taking the logarithm of s to be uniformly distributed, rather than s itself, each value s will be $1/s$ times as likely as before. To still get the same expectation, we have to multiply each value by s . Hence, we are finally left with estimating the expectation of the following process:

Chose $\sigma = \ln s$ uniformly at random in the interval $[\ln(a), \ln(b)]$. Randomly generate a loop of size e^σ and count $(1 - n)e^{-4\sigma} = (1 - n)s^{-4}$ if loop hits $n \geq 2$ elements, and 0 otherwise.

2.4 Symbolic Integration over the Scaling Factor

It makes sense to try to perform at least part of the integration needed to evaluate eq. 2 symbolically, for two independent reasons. While this may on the one hand help to simplify the problem, it also gives us a much more useful handle on problems that involve changing geometries. As we are much more interested in Casimir forces (and moments) than just energies, this is obviously desirable.

In particular, we can, as in [16], typically perform the integration over the loop scaling factor $\int_{s=0}^{\infty} \frac{ds}{s^5} \Theta(sy, x)$ symbolically.

If we have sampled a loop y , we can compute for each sampling point the values of s for which this sampling point is inside a given object. Often, this is just an interval, or at worst the union of a few intervals. By merging these intervals for each sampling point, we can compute the set of s values for which the loop hits the given object. Now, as Θ counts the number of objects hit by the loop, it is piecewise constant on the partitioning so obtained; if $\Theta = n$ for $T \in [a, b]$, we have $\int_a^b \frac{ds}{s^5} \Theta(sy, x) = n(a^{-4} - b^{-4})/4$.

Note that this means that we also do not need to specify the region of s which we want to sample, i.e. our method does not need to know a geometric length-scale.

2.5 Forces on Multiple Bodies via Sensitivity Backpropagation

In order to calculate forces, we have to determine by how much Casimir energies change when changing the geometry. Taking the limit $\Lambda \rightarrow \infty$, the subtraction scheme eq.10 is only compatible with geometry changes that change the position and orientation, but not shape, of individual bodies: evidently, the Casimir energy attributed to a single body via this scheme is zero, regardless of its shape. As we naturally would expect the Casimir force between two parallel flat plates to not disappear when connecting them with a thin wire (so that they become a single object), the regularization prescription that amounts to attributing forbidden loops to specific objects cannot be compatible with (unconstrained) shape changes.

Even if we limit ourselves to shifts and rotations of bodies, retaining eq. 10, it makes sense to describe geometry changes in a more general way. We hence consider the potential V to be a function of multiple geometry parameters (positions and angles), e.g. $V = V(r_1^a, r_2^a, r_3^a, r_1^b, r_2^b, r_3^b, \alpha_1^a, \beta_2^a, \gamma_3^a; \dots)$.

If we perform integration over the scaling parameter s analytically for every loop and consider the intervals over which the subset of objects pierced by that loop does not change, then the interval endpoints, will become analytic functions of the geometry parameters – and so will the loop’s contribution to the total Casimir energy.

For any given loop, we have to perform a fairly simple computation, which in the end gives a single number. Furthermore, it is perfectly feasible to design the algorithm in such a way that at the end of the computation of the loop’s contribution to the Casimir energy, we still remember all the intermediate values that entered that calculation. In such a situation, there is a standard method (in the sense of an algorithmic transformation on the program that calculates the loop energy) that allows a fast evaluation of the gradient with respect to all the geometry parameters. Irrespective of the number N of such parameters, and the complexity of the intermediate expressions, it is possible to obtain the gradient to full numerical accuracy with at most 5 times the computational effort needed to calculate the scalar function (often even much less). In comparison, the naive direct method of calculating the gradient by comparing function values would require at least $N + 1$ full evaluations of the function (and then only give a result with reduced numerical accuracy).

The generic approach that makes this possible, which has become known under the names “automatic/algorithmic differentiation”, “sensitivity backpropagation”, or “adjoint code” [17, 18] is essentially based on this idea:

- Every intermediate result used in the calculation gets stored away for later use (i.e. none may be dropped or over-written).
- To each such intermediate quantity I_k stored, we associate a buffer that can store another number \bar{I}_k , initialized to zero at the beginning of the program. Ultimately, these will each end up holding the answer to the question: “If, at the point when I_k became first known during the calculation of the function value, we interrupted the computation, changed that value from I_k to $I'_k = I_k + \epsilon$, and then allowed the computation to proceed without further modifications now using I'_k instead of I_k , by how much would the final result then change, relative to ϵ (in the limit of small ϵ)?”. Hence, the \bar{I}_k will eventually become *sensitivities* that describe the dependence of the result on the given intermediate quantity.
- Treating input parameters in the same way as intermediate values, the sensitivities on all the input values give the function’s gradient.
- Sensitivities are calculated in a two-step process: first, the function is evaluated once to obtain all the intermediate quantities for the given choice of input parameters. Then, starting from the result, which has been obtained from an arithmetic operation involving intermediate values, sensitivities for the last intermediate get updated. As these again have been the result of some arithmetic operation, the sensitivities for the intermediate values they have been obtained from can be determined, etc. As one intermediate quantity may be used multiple times throughout the calculation, it is important to collect incremental contributions to sensitivities when going backwards through the computation.

The theoretical maximum effort factor of 5 can be traced back to the effort required to handle multiplication/division of intermediate values. Evidently, if the sensitivity of the result on the intermediate quantity I_k is known in \bar{I}_k , and I_k was obtained as the sum of $I_i + I_j$, then the sensitivities of I_i and I_j must be increased by \bar{I}_k (for if e.g. I_j gets used multiple times, then \bar{I}_j receives multiple increments). If, however, I_k is the *product* of I_i and I_j , then \bar{I}_i must be increased by $I_j \cdot \bar{I}_k$ and vice

versa – the combined read/add/store operations give rise to a bounded multiplicative factor for the total effort.

In practice, the corresponding calculations are even considerably simpler than what the general theory of algorithmic differentiation suggests, as the partial derivatives $\partial E/\partial g_j$ with respect to the geometry parameters g_j are, at least for simple surfaces, obtainable directly as a by-product of the forward calculation. Comparing the Worldline method with the remarkable approach discovered by Rodriguez, Ibannescu, Iannuzzi, Capasso, Joannopoulos, and Johnson [19, 20] or for that matter any method that involves numerically solving discretized sparse linear operator equation systems, one would naturally not expect sensitivity backpropagation to be as readily applicable with these approaches as with Worldline Numerics. On the one hand, sensitivity backpropagating an iterative linear solver would require remembering the intermediate values from all iteration steps (otherwise thrown away), and also, the calculation may have happened to produce a solution before having explored some of the dependencies sufficiently well. While research has been done on backpropagating linear solvers, the incorporation of this strategy into Worldline Numerics undeniably is much easier to accomplish.

2.6 Adaptive Sampling

In a typical geometry, essentially the whole energy or force is contributed by few, comparably small regions. These are typically the regions where two objects come closely together.

While we still have to sample loops in such a way that we integrate over all of the relevant region of space, it is worthwhile to focus effort mainly on these highly contributing areas, as the absolute uncertainty of our Monte-Carlo estimation is much higher there. We achieve this in the following way: We first specify an absolute accuracy to which we want the density estimated to at every point. When later sampling the density at a given point, we first take a specified minimum of samples. From that we estimate the (unbiased) variance of our sampling at this point. We continue sampling until a pre-defined (95%) confidence interval for the sampling mean is smaller than the prespecified accuracy.

2.7 Living with Cancellation

Some geometries, like the “cylinders with sidewalls” geometry studied in [21], show a high degree of symmetry. While perfect symmetry helps to reduce the computational effort as the calculation can be restricted to a fundamental domain, slightly non-symmetric configurations often are a problem if we want to compute the force on an object that gets pulled in different (perhaps opposing) directions: most of the contributions cancel, giving rise to a small residual force.

A naive approach would compute the contribution at both sides of the object separately and then add up. This, however, would yield a huge variance for a comparably small resulting value. Fortunately, the force contribution of a loop and its mirrored image are highly correlated in these situations. Often, one is the negative value of the other. So we have a better way of estimating the contribution by estimating the expectation of the following process:

Randomly pick a loop and also consider its mirror image under the symmetry; then add up the force contributions of both these loops.

In that way, we do not change the expectation value of the sum, but, due to the correlation, the variance is much smaller. In that way, it is possible to compute force contributions where a naive approach would require excessive effort due the huge variation, as in the system discussed in Section 3.

2.8 Parallelization

In the Worldline formalism the calculation of contributions to the total energy (or force) can be performed independently for each grid point. Also, for each grid point, the contribution of each loop to the energy (or force) does not depend on the contribution of the other loops. Thus the problem is easily seen as being embarrassingly parallel, and furthermore the basic component – processing a loop – does not require overly complex calculations (in the sense of memory requirements and algorithmic effort). As the worldline method is a probabilistic approach, the accuracy of the calculation can be increased (within reasonable limits dictated by computational effort) by increasing the number of grid points, number of loops, and the number of points per loop in an appropriate way.

As the computation for each point and loop follows the same algorithm, this approach fits the SIMD (single instruction, multiple data) processing approach very well. Powerful massively parallel

```

while (stacksize>0) {
    pop(StartPos, EndPos, &level);
    if (level > 0){
        MidPos = (StartPos + EndPos) / 2 + gauss_normal(0, sigma(level));
        push(MidPos, EndPos, level-1);
        push(StartPos, MidPos, level-1);
    }
    else calc_contribution(StartPos);
}

```

Figure 2: Schematic structure of the code managing a stack of yet-to-be-split arcs.

SIMD hardware is now available at a highly competitive price in the form of specialized Graphics Processing Units (GPUs), where development has – to a large extent – been driven by the video game industry.

When implementing Worldline Numerics on GPU hardware, one has to bear in mind certain constraints of GPU programming. The memory hierarchy of most GPUs discerns between global memory and a special form of fast local memory called “shared memory”. It is often favourable to perform most of the computations in shared memory. This fast shared memory typically is quite small and has to be divided between simultaneously running work items, thus limiting the number of loop points that can be computed concurrently. One also has to keep in mind that GPUs perform rather poorly on complex branching patterns and the hardware optimizations on GPUs mainly target a high throughput of floating point operations, often neglecting the performance on integer calculations needed for most Pseudo Random Number Generators (PRNGs).

On account of shared memory size limitations, the authors developed a version of the d-loop algorithm that generates, for each loop, the loop points on the fly – without ever storing the entire loop in memory. As GPUs do not support recursion directly, it is advantageous to instead manage a stack of arcs yet to be split in half, as sketched in figure 2.

This manages to reduce the memory footprint of loop generation and processing from $\mathcal{O}(N)$ to $\mathcal{O}(\log(N))$, N being the number of loop points. This makes it possible in principle to shift loop generation to GPU cores even for loops too large to fit into the shared GPU memory. In most cases, however, it seems more appropriate to instead pre-generate loop shapes on the CPU and subsequently upload them into GPU read-only memory visible to each GPU work item. The GPU threads then perform intersection checks for loops of pre-determined shape shifted to different grid points. Using the same set of loops at all grid points also helps in terms of statistics as there then can be direct cancellation between opposing forces arising from similar geometric structures. (See also the discussion in Section 2.7.)

The authors so far used GPUs mainly with the direct numerical integration method described in section 2.3 and have at the time of this writing not yet generalized the (algorithmically much less uniform) handling of scale factor intervals to the GPU for different geometries. First computations in the plate-plate geometry show a much better convergence than a full Monte-Carlo integration.

As language for the implementation of the algorithm the authors have used OpenCL in combination with PyOpenCL[22]. This helps code re-use across a broad spectrum of multi- or manycore architectures.

2.9 Generalization to Electrodynamics?

While Worldline Numerics has drawbacks in comparison to other computational approaches, such as e.g. its inability to easily incorporate frequency-dependent optical properties of immersion media, it also has, from an applications perspective, some potentially very attractive characteristics (as we have reasoned out in this article). The biggest present obstacle to the utilization of Worldline Numerics for engineering applications is that it has not yet been generalized from (massless and massive) scalar fields to photons interacting with conductors. As we demonstrate in section 3, trying to use scalars to approximate the behaviour of photons can easily give qualitatively wrong results – so, the need to be able to handle photons is quite pressing from an application perspective.

While worldline methods can in principle be adopted to dealing with vector bosons, as has been explored e.g. in [23] for gluon loop radiative corrections, the challenge is in properly modeling the boundary conditions for photon-conductor interaction. Considering the structure of the theory, one would at least expect that it should be achievable to couple the photon to a charged scalar undergoing spontaneous symmetry breaking, giving it an effective mass inside each object. This would then amount to modeling electromagnetic Casimir forces in the presence of superconductors.

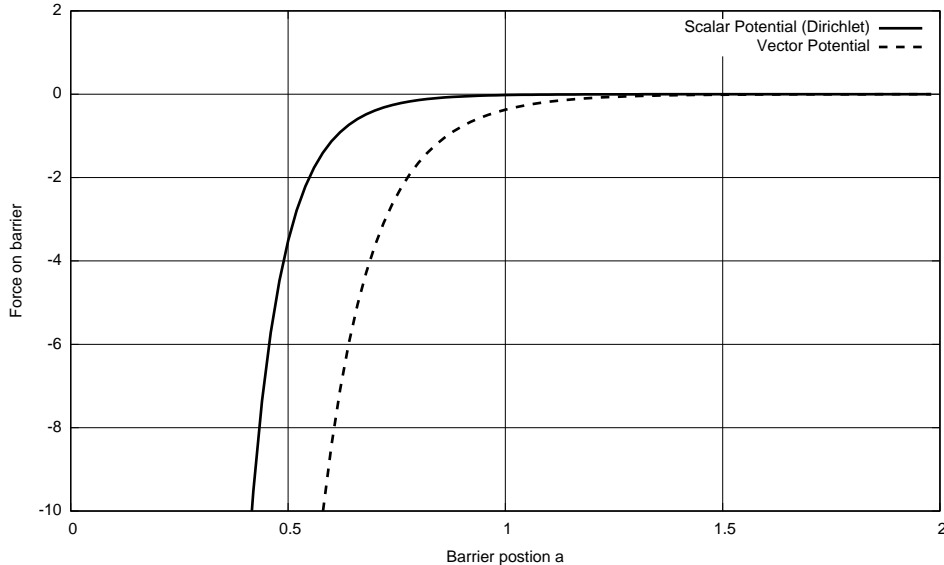


Figure 3: Casimir forces in the piston geometry as a function of barrier height, calculated for scalars and photons using the analytic expressions given in [24].

Rather than trying to construct a generalization of Worldline Numerics for photons and conductors starting from quantum electrodynamics principles, we for now approach this problem in a more adventurous way, if only to generate ideas: here, our guiding question is what the simplest conceivable generalization of Worldline Numerics might be that could possibly stand a chance of modeling electrodynamics. Naturally, the subsequent discussion in this section will be of highly speculative nature.

Obviously, such a generalization will involve having photons propagate in loops. As we are not particularly interested in manifest Lorentz invariance here, we may just as well straightaway choose to gauge away the non-dynamic timelike component of the electromagnetic vector potential A_0 , leaving us with a three-dimensional vector describing the photon polarization state. This is, of course, still redundant, as the photon only has two (transversal) physical states rather than three, but it might be conceivable to ultimately end up with a formulation in which, after evaluating the integrals over loop shapes and sizes, it turns out that the boundaries do not interact with (i.e. never see) the longitudinal photons. In such a case, they would drop out from all Casimir forces.

It makes sense to assume that, as in the scalar case, bodies can be modeled as hollow thin shells; if we accept the perfect conductor approximation (which in particular states that characteristic length scales from the geometry are large in comparison to characteristic atomic distances), we would not expect to be able to probe the inner structure of conductors by looking at Casimir forces between them. So, we need to only concern ourselves with what happens when a photon loop pierces a conductor surface. The boundary conditions of a perfect conductor ($\vec{n} \times \vec{E} = 0$ – no electric field parallel to surface, as this would immediately be compensated by charges shifting accordingly, and $\vec{n} \cdot \vec{B} = 0$ – no magnetic field perpendicular to surface, as this would be compensated by eddy currents, at least for frequencies ω sufficiently large for the perfect conductor approximation to hold) have to be implemented in some way. We want to consider all possible (including un-physical longitudinal) photon polarizations simultaneously, and hence should associate to every loop edge a 3×3 matrix acting on the polarization state. In the end, the contribution to the Casimir energy from the loop under consideration should be taken to be the trace of the product of all these matrices; free propagation will amount to the identity, and the matrix corresponding to an edge that pierces a conductor surface would involve a projection eliminating some polarizations. What form may such a projection matrix have? As we already accounted for photon polarization directions, the only directions available are the surface normal \vec{n} , as well as the local velocity \vec{y} . The $\vec{E} = \partial_t \vec{A} \sim \omega \vec{A}$ condition only involves perpendicularity to \vec{n} , and while the \vec{B} -condition would be expected to pick up spatial components of \vec{y} , re-scaling these in order to form a projector seems to also bring us to a $\vec{A} \perp \vec{n}$ condition, which means that one should take as projector that restricts to forbidden states the matrix $I - \vec{n} \otimes \vec{n}$. Evidently, in the case of parallel plates, the trace would just introduce a factor two relative to the scalar field, as desired.

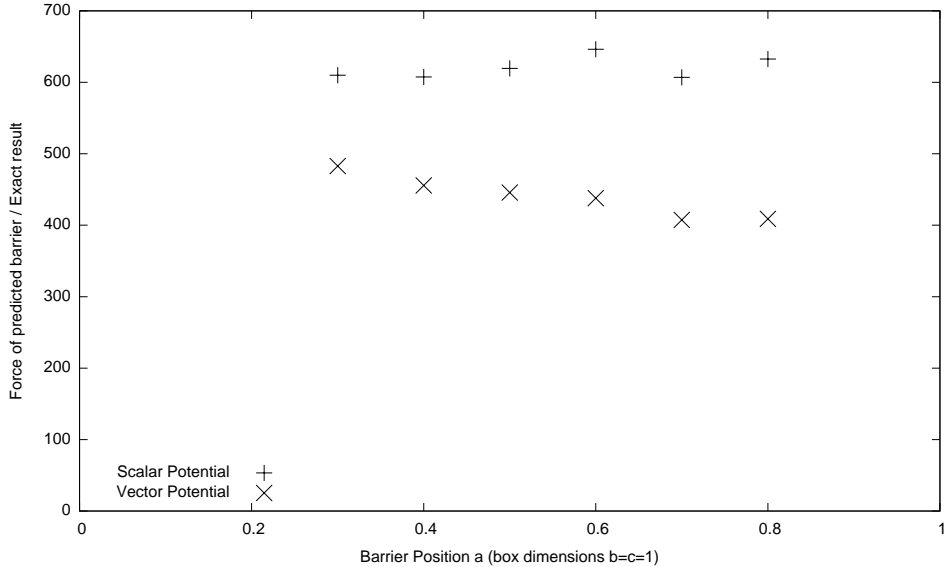


Figure 4: Comparison of predicted forces in the Casimir Piston geometry: The graph shows the ratio of the Casimir forces computed with our method to the exact, analytically computed, values [24], see Figure 3. This ratio is plotted for computations based on scalar fields (upper curve) and photons (lower curve). A constant ratio would indicate perfect coincidence of the methods; note that constant scaling factors (e.g., due to fundamental constants of physics) have not been taken into account in our computations, as they were only carried out to test the functional dependency.

The prescription described above seems, at the superficial level, quite obviously wrong – this is most easily seen by considering a loop close to a box corner made up of different objects: if it pierces three mutually perpendicular faces, it would contribute three forbidden polarizations, where the physical photon only has two. Still, it is valid to ask whether this loop processing prescription is related to some idealization of boundaries in a quantum field theory of vectors – and ask what it might look like.

One would, for the reason given above, naturally expect such a prescription to give energies that do not have much in common with photon Casimir energies. An attractive nontrivial test geometry for which scalar and photon Casimir forces are known exactly, where discrepancies could reasonably be expected to manifest, and in which this scheme is easily implemented, is the piston geometry studied in [24]. If we plot the quotient of the (not yet properly normalized) energies predicted by Worldline Numerics and the analytic result for the scalar field, we get curve 1 in figure 4. If we compute the same ratio for our adventurous “Vector Worldline” generalization and the known result for photons, we get curve 2.

We consider a coordinate aligned closed box with square cross section of side length $b = c = 1$ and height $h \gg b$ – here, we choose $h = 100$. This box is sub-divided by a coordinate-aligned box-shaped movable barrier of identical cross section and infinitely small thickness; the distance between barrier and base of the box is taken to lie in the interval $[0; 1]$.

The spatial sampling of loop positions was done on a Cartesian grid with lattice spacing 0.05, covering a coordinate-parallel cube of edge length 3 centered at the point 0.5 above the center of the box base plate. Forces have been calculated for barrier heights from 0.3 to 0.8 in steps of 0.1, using a central difference quotient with $\delta h = 0.1$.

Since the barrier is taken as being as wide as the box, there is no positive minimum to the contributing loop size. However, for loops much smaller than the distance between barrier and base of the box the local geometry on either side of the barrier symmetric. So the contribution of sufficiently small loops cancels out. In order to avoid infinities, the loop scaling factor s was constrained to the range $[0.02; 6]$ and sampled as described in Section 2.3.

In this system, one must keep in mind that, for the distances involved, Casimir energies, both in the scalar and photon case, vary by more than three orders of magnitude – as shown in Figure 3. While the ratio clearly shows some drift for the photon case in this experimental calculation, it cannot yet be excluded that this may be a discretization related artefact. Given that the simplistic ansatz proposed here would be expected to quite clearly show up as being deeply wrong (considering the ratios involved), this outcome is somewhat remarkable. At the very least, it seems to make sense to

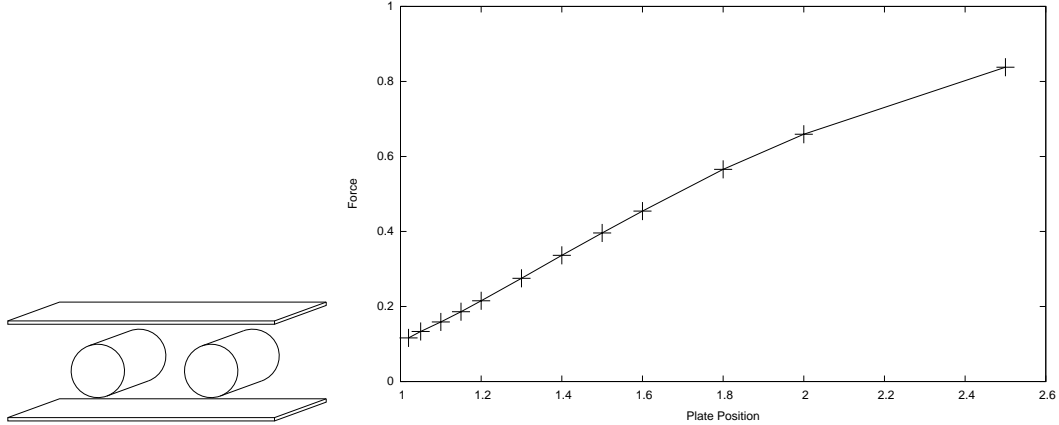


Figure 5: The “cylinders with sidewalls” geometry and the dependency of the attractive scalar Casimir force between the cylinders on the Position of the plates. At position 1.0, the plates would touch the cylinders.

try and explore a small number of other geometries to learn whether this is a curious coincidence for this particular geometry (as one would expect), whether some not yet understood crazy cancellations may actually make this method work as a model for photons (unlikely), or whether it may turn out as being somewhat useful pragmatically in the sense of a heuristic engineering method that is known to be mathematically flawed (as many such engineering heuristics are), but manages to give a reasonably good estimate for some applications.

3 Parallel Cylinders between Plates, revisited

The “cylinders with sidewalls” geometry studied in [21] (Figure 5, on the left) has been shown to nicely demonstrate that Casimir forces are essentially multi-body forces. It is given by two parallel, infinitely long cylinders between two parallel infinite plates. Focusing on the attractive force between cylinders, one finds that this depends in a fairly subtle way on the distance between the plates.

For the calculation whose results are shown in figure 5, the cylinders used have radius 1.0 and centres at (x, y) -coordinates $(-2.0, 0.0)$ and $(2.0, 0.0)$, respectively. The plates are given by the equation $z = p$, where p is varied in the range $1.02 \dots 2.50$. The calculation of the force on the left cylinder used the scaling method, sampling around a grid with spacing 0.05 and exploiting the mirror method (Section 2.7) by taking a reflection-symmetric loop ensemble w.r.t. the plane $x = -2.0$ to reduce the variance due to cancellation. This sampling was done in an adaptive manner (Section 2.6). In total, between $1.9 \cdot 10^7$ and $3.9 \cdot 10^7$ loops of 2^{13} points were sampled for each geometry.

The results are shown at the right-hand side of Figure 5. As opposed to methods such as the proximity force approximation, we do see a dependency of the forces on the cylinder on the plate distance. We however could not find the non-monotonic behaviour reported in the literature [21]. So, once again, we have an example where scalars behave in a qualitatively different way than photons [24].

4 Conclusions

From a microsystems engineering perspective, the Worldline Numerics / Loop Cloud Method has a number of attractive properties, such as the ability to quickly give crude estimates, considerable potential to solve geometric optimization related problems, and of course its conceptual simplicity and intuitiveness that make it a useful educational tool with the potential to give a simple yet quantitatively correct mental model of the origin of Casimir forces. Quite remarkably, the operational procedure can be explained using very simple concepts only – in fact, even without having to use much linear algebra.

At present, the biggest obstacle to its utilization for engineering applications is the method’s inability to handle photons in the presence of conducting boundaries instead of scalar particles in the presence of Dirichlet boundary conditions. As we have demonstrated in section 3 through an example calculation, the problem is that any attempt to use scalars in order to approximate photon

Casimir forces is questionable as this can easily give predictions that are wrong already at the qualitative level.

In addition to this calculation, and to discussing some methodological improvements of the Loop Cloud Method, this article provided some early speculation on whether a simple extension of the method may be able to give useful estimates for photon Casimir forces; despite obvious conceptual issues, the accompanying computation turned out to produce numbers that match the known exact result remarkably well, in particular considering that Casimir forces range over a few orders of magnitude for the problem studied. Still, one naturally would next try to refute the viability of this simplistic approach by checking its predictions for another not too trivial geometry, before starting any attempt to formally prove its validity.

Acknowledgments It is a pleasure to thank Holger Gies and Roman Zwicky for useful discussions and comments on this subject. CPU calculations have been performed on the University of Southampton’s Iridis3 cluster and the LOEWE-CSC cluster of the Goethe Universität Frankfurt. GPU calculations have been performed on the LOEWE-CSC cluster of the Goethe Universität Frankfurt. J. Gerhard received funding for this project by the HGS-HIRE Abroad programm of the *Helmholtz Graduate School for Hadron and Ion Research*. Financial support by the UK Engineering and Physical Sciences Research Council under EPSRC Grant EP/H049924/1 is gratefully acknowledged.

References

- [1] Hendrik Brugt Gerhard Casimir. On the attraction between two perfectly conducting plates. *Proceedings of the Royal Netherlands Academy of Arts and Sciences*, 51(7):793–795, 1948.
- [2] U. Mohideen and Anushree Roy. Precision measurement of the casimir force from 0.1 to 0.9 μm . *Phys. Rev. Lett.*, 81:4549–4552, Nov 1998.
- [3] A. Scardicchio and R. L. Jaffe. Casimir Effects: An Optical Approach I. Foundations and Examples. *Nucl. Phys.*, B704:552–582, 2005, quant-ph/0406041.
- [4] L. Moyaerts, K. Langfeld, and H. Gies. Worldline Approach To The Casimir Effect. *ArXiv High Energy Physics - Theory e-prints*, November 2003, arXiv:hep-th/0311168.
- [5] Sahand Jamal Rahi, Thorsten Emig, and Robert L. Jaffe. Geometry and material effects in Casimir physics - Scattering theory. 2010, 1007.4355.
- [6] Alejandro Rodriguez, Mihai Ibanescu, Davide Iannuzzi, J. D. Joannopoulos, and Steven G. Johnson. Virtual photons in imaginary time: Computing exact casimir forces via standard numerical electromagnetism techniques. *Phys. Rev. A*, 76:032106, Sep 2007.
- [7] H. Gies and K. Langfeld. Loops and Loop Clouds - A Numerical Approach to the Worldline Formalism in QED. *International Journal of Modern Physics A*, 17:966–976, 2002, arXiv:hep-ph/0112198.
- [8] H. Gies and K. Klingmüller. Quantum energies with worldline numerics. *Journal of Physics A Mathematical General*, 39:6415–6421, May 2006, arXiv:hep-th/0511092.
- [9] A. W. Rodriguez, A. P. McCauley, J. D. Joannopoulos, and S. G. Johnson. Casimir forces in the time domain: I. Theory. *ArXiv e-prints*, April 2009, 0904.0267.
- [10] A. P. McCauley, A. W. Rodriguez, J. D. Joannopoulos, and S. G. Johnson. Casimir forces in the time domain: Applications. *Physical Review D*, 81(1):012119–+, January 2010, 0906.5170.
- [11] T. Nagami, H. Mizuta, N. Momo, Y. Tsuchiya, S. Saito, T. Arai, T. Shimada, and S. Oda. Three-dimensional numerical analysis of switching properties of high-speed and nonvolatile nanoelectromechanical memory. *Electron Devices, IEEE Transactions on*, 54(5):1132–1139, may 2007.
- [12] H. Gies, K. Langfeld, and L. Moyaerts. Casimir effect on the worldline. *Journal of High Energy Physics*, 6:18–+, June 2003, arXiv:hep-th/0303264.
- [13] Joao Luiz Dibl Comba and Jorge Stolfi. Affine arithmetic and its applications to computer graphics. *Anais do VII Sibgraphi*, 1993.
- [14] A. Knoll, Y. Hijazi, A. Knesler, M. Schott, Hansen C., and Hagen H. Fast ray tracing of arbitrary implicit surfaces with interval and affine arithmetic. *Computer Graphics Forum*, 28(1):26–40, 2009.
- [15] H. Gies, J. Sánchez-Guillén, and R. A. Vázquez. Quantum effective actions from nonperturbative worldline dynamics. *Journal of High Energy Physics*, 0508, 2005, hep-th/0505275.

- [16] Holger Gies and Klaus Klingmuller. Worldline algorithms for Casimir configurations. *Phys. Rev.*, D74:045002, 2006, quant-ph/0605141.
- [17] B. Speelpenning. Compiling fast partial derivatives of functions given by algorithms. Technical Report COO-2383-0063; UILU-ENG-80-1702; UIUCDCS-R-80-1002, Illinois Univ., Urbana (USA). Dept. of Computer Science, 1980.
- [18] Andreas Griewank. On automatic differentiation. In *IN MATHEMATICAL PROGRAMMING: RECENT DEVELOPMENTS AND APPLICATIONS*, pages 83–108. Kluwer Academic Publishers, 1989.
- [19] A. Rodriguez, M. Ibanescu, D. Iannuzzi, F. Capasso, J. D. Joannopoulos, and S. G. Johnson. Computation and Visualization of Casimir Forces in Arbitrary Geometries: Nonmonotonic Lateral-Wall Forces and the Failure of Proximity-Force Approximations. *Physical Review Letters*, 99(8):080401–+, August 2007, 0704.1890.
- [20] A. Rodriguez, M. Ibanescu, D. Iannuzzi, J. D. Joannopoulos, and S. G. Johnson. Virtual photons in imaginary time: Computing exact Casimir forces via standard numerical electromagnetism techniques. *Physical Review D*, 76(3):032106–+, September 2007, 0705.3661.
- [21] S. J. Rahi, A. W. Rodriguez, T. Emig, R. L. Jaffe, S. G. Johnson, and M. Kardar. Non-monotonic effects of parallel sidewalls on Casimir forces between cylinders. *Physical Review D*, 77(3):030101–+, March 2008, 0711.1987.
- [22] Andreas Klöckner, Nicolas Pinto, Yunsup Lee, B. Catanzaro, Paul Ivanov, and Ahmed Fasih. PyCUDA and PyOpenCL: A Scripting-Based Approach to GPU Run-Time Code Generation. Technical Report 2009-40, Scientific Computing Group, Brown University, Providence, RI, USA, November 2009.
- [23] C. Schubert. Perturbative quantum field theory in the string-inspired formalism. *PHYSREP*, 355:73–234, December 2001, arXiv:hep-th/0101036.
- [24] M. P. Hertzberg, R. L. Jaffe, M. Kardar, and A. Scardicchio. Casimir forces in a piston geometry at zero and finite temperatures. 76(4):045016–+, August 2007, 0705.0139.